ORIGINAL PAPER

Theoretical aspects of binary and ternary complexes of aziridine···ammonia ruled by hydrogen bond strength

Boaz G. Oliveira · Regiane C. M. U. Araújo

Abstract B3LYP calculations, ChelpG atomic charges, and quantum theory of atoms in molecules (QTAIM) integrations were used to investigate the binary (1:1) and ternary (1:2) hydrogen-bonded complexes formed by aziridine (1) and ammonia (2). In a series of analysis, geometry data, electronic parameters, vibrational oscillators, and topological descriptors were used to evaluate hydrogen bond strength, and additionally to determine the more prominent molecular deformations upon the formation of $C_2H_5N \cdots NH_3$ (1:1) and $C_2H_5N \cdots 2NH_3$ (1:2) systems. Taking a spectroscopic viewpoint, results obtained from analysis of the harmonic infrared spectrum were examined. From these, new vibrational modes and red- and blue-shifts related to the stretch frequencies of either donors or acceptors of protons were identified. Furthermore, the molecular topology of the electronic density modeled in accord with QTAIM was absolutely critical in defining bond critical points (BCP) and ring critical points (RCP) on the heterocyclic structures. Taking all the results together allowed us to identify and characterize all the N···H hydrogen bonds, as well as the strain ring of the aziridine and its stability.

B. G. Oliveira (✉) · R. C. M. U. Araújo
Instituto de Ciências Ambientais e Desenvolvimento Sustentável,
Universidade Federal da Bahia,
47801-100 Barreiras, Brazil
e-mail: boazgaldino@gmail.com

R. C. M. U. Araújo
Departamento de Química, Universidade Federal da Paraíba,
58036-300 João Pessoa, PB, Brazil

Introduction

In recent decades, the importance of molecular geometry has been demonstrated widely in many fields of chemistry, especially those in which the main goal is the characterization of intermediaries in chemical reactions [1–6]. In regards to heterorings, for instance, some time ago Holubka et al. [7] proposed a reaction mechanism for the interaction between oxirane (C_2H_4O) and ammonia (NH_3). Later, Banks published two investigations [8, 9] about the reactivity of three-membered rings with nucleophiles, such as ammonia. It is well-known that the stabilization of heterorings is determined by the strain exerted on them [10], which basically provides a high energy rearrangement of atoms, not only in regards to C_2H_4O, but also thiirane (C_2H_4S) and aziridine (C_2H_5N).

Although the strain energy is considered a destabilizing effect [11] that can be suppressed by the ring-opening reaction promoted by the attack of electrophilic or nucleophilic agents [12, 13], the existence of hydrogen bonds is of course one of the cornerstone events in this regard [14–18], as recently revisited by Takahashi et al. [19]. It is worth remembering that, by definition, the classical model of the hydrogen bond takes into consideration one stable interaction between a center with high electronic density and a proton donor, such as a lone-electron pair or unsaturated bond and a Lewis acid [20–23], respectively. From a theoretical standpoint, among the large number of computational studies published in recent years [24], we would like to emphasize one specific work that paid great attention to the occurrence of hydrogen bonds in

the binary systems formed by thiirane and ammonia [25]. On the other hand, it has also been reported that binary hydrogen complexes are not dominant structures, since ternary complexes are also important for a thorough analysis of reaction mechanisms [26]. In practice, it is well known that ternary complexes are more stable than binary ones because stronger or multiple hydrogen bonds [27] as well as dihydrogen bonds [28–30] are formed, as reported by Jursic [31], Grabowski [32, 33], Biczysko and Latajka [34], and others [35, 36].

In concordance with the experimental works of Caminati et al. [37] and Mäder et al. [38], which have shown that ammonia acts as a proton acceptor, it remains important to know whether aziridine and ammonia can be efficient proton donors/acceptors when binary ($C_2H_5N\cdots NH_3$) and ternary ($C_2H_5N\cdots 2NH_3$) hydrogen-bonded complexes are formed. In this context, it is important to remember that binary hydrogen complexes formed by aziridine and Lewis' acids are more stable than those whose proton acceptors are oxirane or thiirane [39–41]. In addition, it is worth noting that the formation of multiple hydrogen bonds leads ammonia to behave bilaterally as either a proton acceptor or donor, although our interest here is restricted to investigating if this condition truly affects stabilization of the hydrogen-bonded complex [42–44]. It is clear that the $C_2H_5N\cdots NH_3$ and $C_2H_5N\cdots 2NH_3$ complexes should be part of the mechanism reaction of the aziridine under proton donor/acceptor attacks and, in this case, two ammonia molecules can act as a Lewis acid or base [45].

Methods

Theoretical level and calculation methods: B3LYP, ChelpG, and QTAIM

In order to obtain results that support the hypothesis outlined above, it is essential to choose computational approaches suitable for modeling hydrogen bonds, in particular those formed between aziridine and ammonia. As such, density functional theory (DFT) [46] was chosen as our standard calculation method because it has been employed successfully in studies of intermolecular systems [47–49]. Using a robust capability test, Xu et al. [50] revealed that B3LYP is a valuable functional in view of the small errors associated with the prediction of the relative binding energies of intermolecular systems [51–53]. In general, although a weak or medium-strength interaction, the formation of hydrogen bonds is supported chemically by the overlapping of the LUMO and HOMO frontier orbitals of the respective donor and acceptor of protons, with a dynamic charge transfer flux occurring

between them [54]. Thereby, it is inappropriate to treat hydrogen bond energies without considering charge transfer measurement [55–57]. In the case of heterocyclic compounds [58, 59], recent studies have shown that ChelpG is an efficient method for quantifying charge transfer to the proton donor upon the formation of hydrogen bonds [60]. Thus, we used ChelpG atomic charge partition in this current work, as we expected that charge transfer quantification would help interpret the function of aziridine and ammonia either as donor or acceptor of protons.

Once again, as our main goal is focused on hydrogen bond characterization, we used the quantum theory of atoms in molecules (QTAIM) [61] to compute the topology of the electronic density in each chemical bond, as well as for all potential interactions existing between aziridine and ammonia. The QTAIM topology was conceived by Bader almost 40 years ago when he grouped a series of quantum-mechanical concepts in order to unveil atomic behavior within molecules [62, 63]. This gave rise to the virial theorem of electronic density, according to which kinetic and potential operators determine and model interatomic topography by taking the electronic density as the quantum observable. Furthermore, topological parameters derived from Bader's analysis have been useful in studies of chemical reactions [64], although the great advantage of QTAIM is attributed to its ability to quantify the electronic density (ρ), which can be found in increased and decreased quantities when its Laplacian is negative ($\nabla^2\rho < 0$) and positive ($\nabla^2\rho > 0$), respectively. So, the negative and positive values of the Laplacian indicate the concentration and depletion of charge density, and this topological condition is governed by the eigenvalues of the Hessian Matrix ($\nabla^2\rho \equiv \lambda_1 + \lambda_2 + \lambda_3$), whereas the electronic density ρ is described as a set of critical points classified as follows: cage critical points (CCP), ring critical points (RCP), bond critical points (BCP), and nuclear attractors (NA). Like the recent observations of Huang et al. [65], we expect that our structural, electronic, topological, and vibrational results could be useful parameters with which to understand the formation of $C_2H_5N\cdots NH_3$ and $C_2H_5N\cdots 2NH_3$ hydrogen-bonded complexes and their hydrogen bond strengths.

Computational details and procedure

The optimized geometries of the $C_2H_5N\cdots NH_3$ and $C_2H_5N\cdots 2NH_3$ hydrogen-bonded complexes were determined at the B3LYP/6-311++G(d,p) level of theory with all calculations performed by the GAUSSIAN 98W program [66]. The arguments of the supermolecule approach [67] were used to determine the values of the hydrogen bond energies (ΔE), which were corrected through the Boys and

Bernardi's basis sets superposition error (BSSE) [68] and thermodynamic results of the zero point energy (ZPE) [69].

The QTAIM calculations were developed in two ways:

(1) Applying the standard procedures of the GAUSSIAN 98W program [70];
(2) Using the interactive AIM2000 1.0 software [71].

In order to obtain the charge transfer, ChelpG atomic charges [72] were calculated using the GAUSSIAN 98W program.

Results and discussion

Structure

From the B3LYP/6-311++G(d,p) calculations, the optimized geometries of the binary $C_2H_5N \cdots NH_3$ (**I**, **II**, and **III**) and ternary $C_2H_5N \cdots 2NH_3$ (**IV** and **V**) hydrogen-bonded systems are depicted in Fig. 1, whereas the results of the most evident structural alterations upon these complexations are given in Table 1. Because the hydrogen bond distance is one of the structural benchmark criteria used to evaluate interaction strength, the longer length of 2.581 Å of the $N \cdots H^b$ hydrogen bond in binary system **III** is relatively large in comparison with the shorter bond lengths of 2.167 Å ($N \cdots H^d$) and 2.197 Å ($N \cdots H^c$) for **I** and **II**, respectively. Therefore, by knowing the bond length value of 1.015 Å for N–H in the ammonia monomer, **I** is the only binary system that revealed an increasing of 1.021 Å in this bond, a variation of 0.006 Å. Thus, the $N–H^d$ bond in **I** seems to be a proton donor site as the hydrogen bond theory affirms that bond lengths of proton donors are altered substantially after complexation [73, 74]. On the contrary, slight variations in the $N–H^d$ bonds of **II** and **III** were observed. Otherwise, aziridine actually operates as a proton donor in **II**, as can be verified by the $N–H^c$ bond length of 1.021 Å, which would be 1.016 Å in the isolated state. Ternary complexes concern mainly **IV**, whose $N \cdots H^d$ interaction length of 2.141 Å is shorter than that found for $N \cdots H^c$ (2.179 Å). If we compare these hydrogen bond

Fig. 1 Optimized geometries of the binary ($C_2H_5N \cdots NH_3$) and ternary ($C_2H_5N \cdots 2NH_3$) hydrogen-bonded complexes obtained through application of the B3LYP/6-311++G(d,p) level of theory
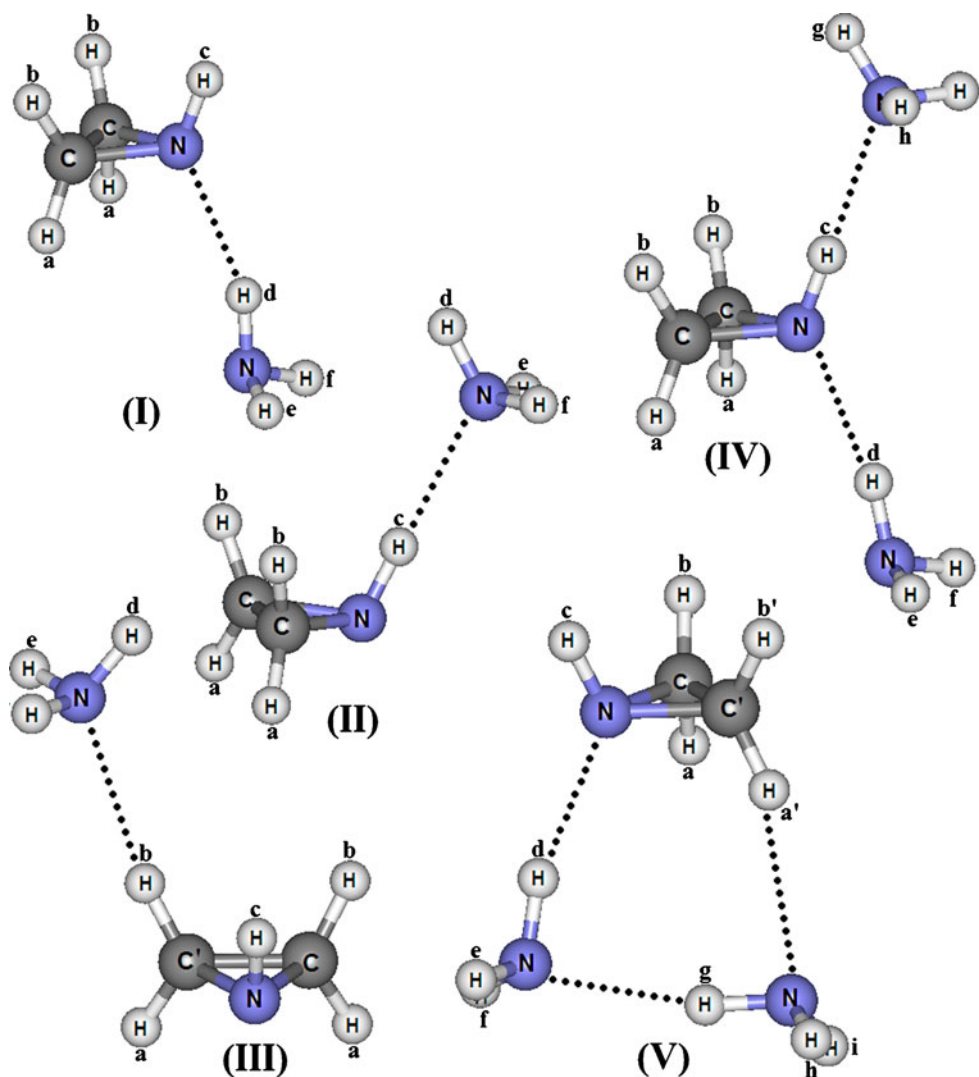
Table 1 Structural parameters of the binary $C_2H_5N\cdots NH_3$ (**I**, **II**, and **III**) and ternary $C_2H_5N\cdots 2NH_3$ (**IV** and **V**) hydrogen-bonded complexes using B3LYP/6-311++G(d,p) calculations. All values are in Ångstroms (Å). Bond length in the ammonia monomer: $N-H = 1.015$ Å; bond lengths in the aziridine monomer: $C-N = 1.472$ Å, $C-H^b = 1.086$ Å, $C-H^a = 1.084$ Å, and $N-H = 1.016$ Å

Parameters	Hydrogen-bonded complexes				
	I	**II**	**III**	**IV**	**V**
$N\cdots H^d$	2.167	—	—	2.141	2.135
$N\cdots H^b$	—	—	2.581	—	—
$N\cdots H^c$	—	2.197	—	2.179	—
$N\cdots H^g$	—	—	—	—	2.190
$N\cdots H^{a'}$	—	—	—	—	2.507
$N-H^d$	1.021	1.015	1.015	1.023	1.025
$N-H^e$	1.014	1.015	1.015	1.014	1.015
$N-H^f$	1.014	1.015	1.015	1.014	1.015
$N-H^g$	—	—	—	1.015(7)	1.024(0)
$N-H^h$	—	—	—	1.015(7)	1.015(5)
$N-H^i$	—	—	—	1.015(7)	1.015(5)
$N-H^c$	1.016	1.021	1.016	1.022	1.016
$C-H^b$	1.085	1.087	1.086	1.086	1.085
$C-H^{b'}$	—	—	—	—	1.086
$C'-H^a$	—	—	1.084	—	—
$C'-H^b$	—	—	1.085	—	—
$C-H^a$	1.084	1.085	1.084	1.084	1.084
$C'-H^{a'}$	—	—	—	—	1.085
$C-C$	1.483	1.486	1.484	1.484	1.483
$C-N$	1.475	1.469	1.473	1.471	1.476
$C'-N$	—	—	1.476	—	1.480

lengths with those examined in **I** and **II**, it can be seen that the shortest interactions occur in **IV**. In fact, it should be remarked that $N\cdots H^d$ is the shortest hydrogen bond, which corroborates protonation of the aziridine [75]. Of course, this is not absolutely conclusive, but it is fair to say that formation of the hydrogen bonds provides some interesting insights into chemical reactivity [76].

Furthermore, a multiple interaction profile can be seen in **V**, in which three hydrogen bonds ($N\cdots H^d$, $N\cdots H^g$, and $N\cdots H^{a'}$) were discovered. As discussed earlier, these hydrogen bonds are certainly shorter in **V** than those computed for binary complex **I**, ternary **IV**, and the $NH_3\cdots NH_3$ dimer. It should be noted that the length of 2.135 Å for the $N\cdots H^d$ hydrogen bond is shorter 0.032 Å and 0.006 Å in comparison to the respective values calculated for **I** and **IV**. In the case of the $NH_3\cdots NH_3$ dimer, the hydrogen bond length of 2.255 Å calculated at the B3LYP/6-311++G(d,p) level of theory is longer than the value of 2.190 Å for **V**. Nevertheless, it should be stated that all hydrogen bonds examined here are in good agreement with sum of the van der Waals radii, which for

hydrogen and nitrogen equals 2.750 Å [77]. Taking an overview, it is very clear that the shortest hydrogen bonds are observed in the ternary hydrogen-bonded complexes, which suggests a stronger hydrogen bond followed by more accentuated stabilization and higher intermolecular energy. This can be confirmed by the longer bond length values of 1.023 Å and 1.025 Å for $N-H^d$, which reflects perfectly the hydrogen bond strengths in **IV** and **V**. As discussed above, increases in the bond length of the proton donors are expected upon complexation, but in the case of the NH_3 and $NH_3\cdots NH_3$, whose N–H bond lengths are 1.015 Å and 1.020 Å, the results of 1.023 Å and 1.025 Å indicate a proton donor profile because significant elongations were observed.

Moreover, some characteristics of systems **III** and **V** should be noted. These are the only systems to form specific hydrogen bonds, where the $C-H^{b'}$ and $C'-H^{a'}$ bonds are the proton donors. Accordingly, the values of 1.086 Å and 1.085 Å observed show that these bonds were less affected than the corresponding $C-H^b$ and $C-H^a$ bonds, which displayed shorter lengths of 1.085 Å and 1.084 Å, respectively. As already discussed, if the hydrogen bond distances are either shorter or longer, indicating slight or drastic alterations in proton donor bond lengths, this will in practice affect their stretching modes directly. However, this is a cornerstone discussion we will come back to later in the analysis of the harmonic infrared spectrum. Before that, it is necessary to return to the structural analysis by focusing on the most critical characteristic of small heterorings: strain structure [78]. According to the specialized literature [79, 80], strain structure is a phenomenon attributed to deformations of C–Y bonds (Y = oxygen, carbon, sulfur, and nitrogen). From the results gathered in Table 1, it can be seen that the C–C bond lengths are not considered as major structural changes on the aziridine ring upon complexation. In spite of this, some interesting information can be gleaned from the values of the C–N bond lengths. Indeed, when studying systems, such as aziridine, with high strain energy, one can ask whether it is natural to assume that the C–N bond length is drastically increased after complexation? In fact, the answer to this is absolutely not, because shortening of the C–N bond length of **II** was observed, i.e.; values of 1.469 Å and 1.472 Å for the C–N bond lengths in the aziridine monomer and in the binary complex **II**, respectively. This is not surprising since **II** is not a typical structure to be protonated, which led us to consider that strain relaxation might not necessarily occur.

Electronic parameters: interaction energy and charge transfer

Table 2 lists the results for the following electronic parameters: electronic energies (E), hydrogen bond energies

Table 2 Values of the total electronic energies (E^T), uncorrected hydrogen bond energies (ΔE), basis sets superposition errors (BSSE), variations in zero point energies (ΔZPE), corrected hydrogen bond energies (ΔE^C) and charge transfer amounts $\Delta QNH_3^{(d\text{-}e\text{-}f)}$ and $\Delta QNH_3^{(g\text{-}h\text{-}i)}$ of the binary $C_2H_5N\cdots NH_3$ (**I**, **II**, and **III**) and ternary $C_2H_5N\cdots 2NH_3$ (**IV** and **V**) hydrogen-bonded complexes using B3LYP/6-311++G(d,p) calculations

Systems	Electronic parameters						
	E^T[Hartree (H)]	ΔE (kJ mol^{-1})	BSSE (kJ mol^{-1})	ΔZPE (kJ mol^{-1})	ΔE^C (kJ mol^{-1})	$\Delta QNH_3^{(d\text{-}e\text{-}f)}$ (e.u.)	$\Delta QNH_3^{(g\text{-}h\text{-}i)}$ (e.u.)
I	−190.55241069	−16.00	1.06	6.11	−7.88	−0.077	—
II	−190.55273604	−16.90	2.46	5.28	−9.16	+0.061	—
III	−190.54908784	−7.32	1.48	3.64	−2.20	+0.064	—
IV	−247.14216984	−34.53	4.87	11.61	−18.05	−0.109	+0.130
V	−247.14384609	−38.93	5.32	14.25	−19.36	−0.046	+0.004

without correction (ΔE), BSSE, variation of the zero point energies (ΔZPE), and hydrogen bond energies with correction (ΔE^C). Initially, it must be assumed that not all E values can be used as stabilization criterion, since the ternary complexes are more concentrated energetically in additive form. However, ΔE^C results are useful for evaluating stabilization, especially because the intermolecular stabilization is one of the main focuses of our discussion. As the basis sets used contain valence (11), diffuse (++) and polarizations (d,p) functions, the BSSE values are smaller than the respective ΔZPE values, which is in accordance with the findings of other studies [81, 82]. Regarding the binary complexes, **III** is, as expected the weaker bonded, while **I** and **II** are, energetically, medium-to-strong bound. Furthermore, **II** is 1.28 kJ mol^{-1} more strongly bonded than **I**, although it has been established structurally that **I** is the preferred intermediate complex. However, this is not true in terms of hydrogen bond energies, by which **II** is the more stable binary complex. It can thereby be assumed that aziridine is the proton donor and ammonia the acceptor. This assumption is backed up by the results of ChelpG charge transfer $\Delta QNH_3^{(d\text{-}e\text{-}f)}$ summarized in Table 2. The values of +0.061 e.u. and +0.064 e.u. show a loss of charge on the ammonia, with these amounts being transferred to aziridine when systems **II** and **III** are formed. In **I**, however, the result of −0.077 e.u. indicates charge transfer flux and shows that aziridine is the proton acceptor and ammonia the donor. Unfortunately, it must be highlighted that the basis of the charge transfer mechanism cannot determine the proton donor/acceptor identity entirely because the electrostatic identity often governs the nature of the hydrogen bond energy [83, 84]. On the other hand, investigation of the charge transfer is thus essential for the interpretation of intermolecular interactions [85], especially as the multiple hydrogen bonds are the cornerstones of the current study.

Regarding the ternary complexes, the hydrogen bond energy of −19.36 kJ mol^{-1} of **V** is higher by only 1.31 kJ mol^{-1} than the respective value found for **IV**. It is especially

important to point out that these ΔE^C values are not the essence of the hydrogen bond strengths because the energies of the **IV** and **V** complexes are uncooperative. In other words, the total energy values of −247.14216984 H and −247.14384609 H cannot be divided equally among the unsymmetrical hydrogen bonds—N···H^d and N···H^c of **IV**, as well as N···H^d, N···H^g, and N···H$^{a'}$ of **V**—as already reported in several studies on the formation of cluster systems [86–88]. The ternary complexes, **IV** and **V**, are formed by two and three hydrogen bonds, respectively, where, in addition to the predominance of the electrostatic potential [89] already quoted here, it is well-known that charge transfer is one of the most important effects in intermolecular interactions [90]. Although $\Delta QNH_3^{(d\text{-}e\text{-}f)}$ charge transfer values of −0.109 e.u. and −0.046 e.u. indicate that ammonia is the proton donor in **IV** and **V**, the $\Delta QNH_3^{(g\text{-}h\text{-}i)}$ values of +0.130 e.u. and +0.004 e.u. show that the second ammonia molecule (hydrogen atoms signed by 'g', 'h', and 'i') is a proton acceptor. This is apparent visually in **IV**, but not in **V**.

Infrared harmonic spectrum: red-shifting and blue-shifting hydrogen bonds

A vibrational analysis of complexes **I**–**V** was carried out to examine the new vibrational modes commonly known as hydrogen bond stretch frequencies, as well as the main alterations in the stretch modes of the proton donors [91], the nature of which may be red- or blue-shift. According to the values summarized in Table 3, weaker new vibrational modes N···H^d, N···H^c, and N···H^b were observed for the binary complexes **I**, **II**, and **III**, where their respective values of 163.2, 138.8, and 96.1 cm^{-1} are active in the infrared spectrum due to their low absorption intensities of 10.3, 2.1, and 1.4 km mol^{-1}. With regards to ternary complexes **IV** and **V**, their stretch frequency values of 186.2 cm^{-1} and 166.6 cm^{-1} and intensities of 25.6 km mol^{-1} and 14.4 km mol^{-1} of the new vibrational modes for N···H^d are significantly higher than for **I**, for which comparative

Table 3 Values of the stretch frequencies (cm^{-1}) and absorption intensities (in parentheses; km mol^{-1}) of the binary C$_2$H$_5$N⋯NH$_3$ (**I**, **II**, and **III**) and ternary C$_2$H$_5$N⋯2NH$_3$ (**IV** and **V**) hydrogen-bonded complexes using B3LYP/6-311++G(d,p) calculations

Modes*	Hydrogen-bonded complex				
	I	**II**	**III**	**IV**	**V**
N⋯H^d	163.2 (10.3)	—	—	186.2 (25.6)	166.6 (14.4)
N⋯H^b	—	—	96.1 (1.4)	—	—
N⋯H^c	—	138.8 (2.1)	—	116.7 (1.8)	—
N⋯H^g	—	—	—	—	159.3 (4.2)
N⋯H$^{a'}$	—	—	—	—	116.3 (9.5)
δ(N–H^d)	−66.9 (72.5)	−3.3 (1.3)	−5.6 (0.6)	−94.8 (124)	−96.1 (107.5)
δ(N–H^e)	—	−3.3 (1.3)	−5.6 (0.6)	—	—
δ(N–H^f)	—	−3.3 (1.3)	−5.6 (0.6)	—	—
δ(N–H^g)	—	—	—	−4.8 (1.0)	−114.7 (92.4)
δ(N–H^h)	—	—	—	−4.8 (1.0)	—
δ(N–H^i)	—	—	—	−4.8 (1.0)	—
δ(N–H^c)	+6 (2.1)	−81.9 (278.2)	—	−91 (298)	−0.7 (1.5)
δ(C'–H^b)	—	—	+88 (0.7)	—	—
δ(C–H^b)	—	—	—	—	0.8 (1.5)
δ(C–H$^{a'}$)	—	—	—	—	0.8 (1.5)
δ(C'–H$^{a'}$)	—	—	—	—	−12.9 (1.9)
υ^{pes}	0	0	1	0	0

* All δ values indicate: (1) variation in the stretch frequency computed in the complex minus its correspondent value in the monomer; (2) the absorption intensity ratios (I,c/I,m), obtained comparing the values in complex (I,c) and monomer (I,m), are listed in parentheses; υ^{pes} number of negative stretching frequencies found by the analysis of the potential energy surface

values of 163.2 cm^{-1} and 10.3 km mol^{-1} were then computed. However, this profile is not found in **II** and **IV**, in which the stretch frequencies of the hydrogen bond N⋯H^c are 138.8 cm^{-1} and 116.7 cm^{-1}, respectively. In fact, there is no conflict because the hydrogen bond N⋯H^c is not preferential in **IV** as the protonation on the aziridine can occur on nitrogen. In complex **V**, in addition to the fact that the stretch frequency of N⋯H^d is also weaker than in **IV** and stronger than in **I**, there are two new vibrational modes N⋯H^g and N⋯H$^{a'}$, whose stretch frequency values are 159.3 cm^{-1} and 116.3 cm^{-1}, whereas the intensities are 4.2 km mol^{-1} and 9.5 km mol^{-1}, respectively.

According to the specialized literature, the new vibrational modes exist solely due to the formation of hydrogen bonding, as demonstrated by the variation in the stretch frequencies and absorption intensities of the proton donors [92]. However, the values reported in Table 3 should be analyzed carefully once the lowest and most significant frequency displacements are obtained for the whole set of aziridine⋯ammonia complexes. Furthermore, complex **I** exhibits a clear red-shift of −66.9 cm^{-1} in the N–H^d bond, and a slight blue-shift of +6 cm^{-1} in N–H^c. Owing to the drastic vibrational displacement in the N–H^d bond, ideally the proton donor function of this bond can be then validated upon formation of complex **I**. On the other hand, a red-shift effect of −81.9 cm^{-1} is observed in the N–H^c bond of complex **II** with an absorption intensity ratio of 278.2, meaning the appearance of traditional hydrogen bond profiles [93], but notably here with the aziridine as proton donor. Moreover, complex **III** is quite unique, with no

vibrational displacements found in NH$_3$, although red-shifts of −5.6 cm^{-1} in the N–H^d, N–H^e, and N–H^f bonds were computed, and a large blue-shift of +88 cm^{-1} was identified in the C′–H^b bond of the aziridine ring. Although it is not common for vibrational red- and blue-shifts to appear simultaneously, except in the studies conducted by Barnes [94], Lin [95], Gejji [96], and others [97–99], once again the aziridine is acting as proton donor and, even though the aforementioned blue-shift is very clear, the hydrogen bond strength indicates that **III** is not the most appropriate structure for the binary aziridine⋯ammonia complex.

In comparison with the result of −66.9 cm^{-1} for **I**, a larger red-shift of −94.8 cm^{-1} was observed in the N–H^d bond of the **IV** complex. Moreover, a more evident increase in the intensity absorption was computed for **IV**, whose value of 124 is almost twice than of 72.5 calculated for **I**. Different from **I** but in accordance with **II**, a red-shift of −91 cm^{-1} in the N–H^c bond of **IV** was identified, which is increased drastically by a ratio of 298, an event found routinely in stronger hydrogen bonds. Therefore, as already discussed above, it is natural that a shorter hydrogen bond length accompanied by a stronger new vibrational mode would lead to more severe deformations of the stretch frequencies and absorption intensities. The vibrational aspects of complex **V** also reveal important information, such as the red-shifts of −96.1 cm^{-1} and −114.7 cm^{-1} in the N–H^d and N–H^g bond can be seen accompanied by their respective intensity ratios of 107.5 and 92.4. These vibrational red-shifts are relevant to aziridine ring protonation as well as to the new intermolecular vibrational mode

of the $NH_3 \cdots NH_3$ within the **V** complex, but the slight red-shift of -12.9 cm^{-1} in the C′–H$^{a'}$ bond is a spectroscopic event indicating that **V** is a cyclic complex formed by three hydrogen bonds, N$\cdots$H^d, N$\cdots$H^g, and N$\cdots$H$^{a'}$, and thereby giving rise to the red-shifts in the N–H^d, N–H^g, and C′–H$^{a'}$ bonds, respectively.

QTAIM topology: BCP and RCP

The analysis of molecular topology in the light of the QTAIM has been one of the most useful theoretical methodologies in recent scientific history [100–104]. Designed by Bader, the QTAIM has been applied successfully in several types of investigation [105, 106], including characterization of hydrogen bonds, where QTAIM is one of the procedures used routinely [107–111]. Very recently, a research group stated that the QTAIM topological condition for recognizing hydrogen bond formation is a BCP with coordinates (3,−1) [112]. The values of the Laplacian of the electronic density organized in Table 4 were computed within this BCP framework. The C–H and N–H sigma bonds were modeled in accordance with negative Laplacian values, $\nabla^2\rho < 0$, which are used to describe high concentrations of charge density. From the intermolecular point of view, it can be seen that all hydrogen bonds were characterized using $\nabla^2\rho > 0$.

Although this is only a qualitative discussion, the electronic densities give us a concise profile of hydrogen bond strength. Figure 2 illustrates all the BCPs and bond paths for complexes **I**–**V** and show clearly the formation of the N$\cdots$H^d, N$\cdots$H^b, N$\cdots$H^c, N$\cdots$H^g, and N$\cdots$H$^{a'}$ hydrogen

bonds, whose electronic density values vary between 0.009 and 0.021 e/a$_o^3$. Figure 3 shows a graph plotting hydrogen bond lengths, R, against their QTAIM electronic densities, ρ. Besides the stronger hydrogen bonds with R and ρ values close to 2.135–2.197Å and 0.018–0.021 e/a$_o^3$, the extreme results of 2.507 Å and 2.581 Å and 0.010 e/a$_o^3$ and 0.009 e/a$_o^3$ for the corresponding N$\cdots$Ha' and N$\cdots$H^b hydrogen bonds indicate the weakness of these interactions, and it can thus be assumed that they are not preferential interaction sites.

Castillo et al. [113] have demonstrated the importance of RCPs in studies of single heterorings, whereas Grabowski [114] has shown that hydrogen bond strength can also be measured using RCP properties. The results of the present study, summarized in Table 5, suggest the existence of two RCPs: (1) within the aziridine ring C–N–C; and (2) resulting from the two ammonia molecules interacting with aziridine C′–N$\cdots$H^d–N$\cdots$H^g–N$\cdots$H$^{a'}$. In the latter case, although the electronic density value of 0.002 e/a$_o^3$ for RCP-2 is quite small, this is an irrefutable argument for the formation of the ternary complex **V**. The content of the RCP-V-1 is related closely to the formation of the complexes, and, in particular, to the stabilization of the strain ring phenomenon of the aziridine. Thus, the electronic density value of 0.204 e/a$_o^3$ in the RCP of the aziridine monomer reflects a loosening of the strain ring in the complexes **I**, **III**, and **V**, in which the correspondent values are 0.203 and 0.202 e/a$_o^3$. In contrast to this, the values of 0.205 e/a$_o^3$ and 0.204 e/a$_o^3$ e/a$_o^3$ for **II** and **IV** supply evidence of no strain ring loosening because the electronic densities at the RCP increased and/or remained

Table 4 Values of the electronic densities ρ (e/a$_o^3$) and Laplacians $\nabla^2\rho$ (in parenthesis; e/a$_o^5$) computed at the bond critical point (BCP) (3,−1) of the binaries $C_2H_5N\cdots NH_3$ (**I**, **II**, and **III**) and ternaries $C_2H_5N\cdots 2NH_3$ (**IV** and **V**) hydrogen-bonded complexes

BCP	Hydrogen-bonded complex				
	I	**II**	**III**	**IV**	**V**
N$\cdots$H^d	0.019(0.060)	—	—	0.020(0.063)	0.021(0.063)
N$\cdots$H^b	—	—	0.009(0.024)	—	—
N$\cdots$H^c	—	0.018(0.054)	—	0.019(0.057)	—
N$\cdots$H^g	—	—	—	—	0.018(0.055)
N$\cdots$H$^{a'}$	—	—	—	—	0.010(0.028)
N–H^d	0.329(-1.538)	0.334(-1.483)	0.334(-1.479)	0.328(-1.540)	0.326(-1.544)
N–H^e	0.329(-1.538)	0.334(-1.483)	—	0.328(-1.540)	0.326(-1.544)
N–H^f	0.329(-1.538)	0.334(-1.483)	—	0.328(-1.540)	0.326(-1.544)
N–H^g	—	—	—	0.334(-1.540)	0.327(-1.541)
N–H^h	—	—	—	0.334(-1.540)	0.327(-1.541)
N–H^i	—	—	—	0.334(-1.540)	0.327(-1.541)
N–H^c	0.339(-1.507)	0.335(-1.585)	—	0.334(-1.588)	0.338(-1.500)
C′–H^b	—	—	0.339(-1.499)	—	—
C–H^b	—	—	—	—	0.280(-0.953)
C–H^a	—	—	—	—	0.283(-0.971)
C′–H$^{a'}$	—	—	—	—	0.286(-0.998)

Fig. 2 Illustration of bond paths, bond critical points (BCP), ring critical points (RCP) of binary ($C_2H_5N\cdots NH_3$) and ternary ($C_2H_5N\cdots 2NH_3$) hydrogen-bonded complexes. *Red spheres* BCP, *yellow balls* RCP, *blue spheres* nitrogen, *black spheres* carbon, *gray spheres* hydrogen
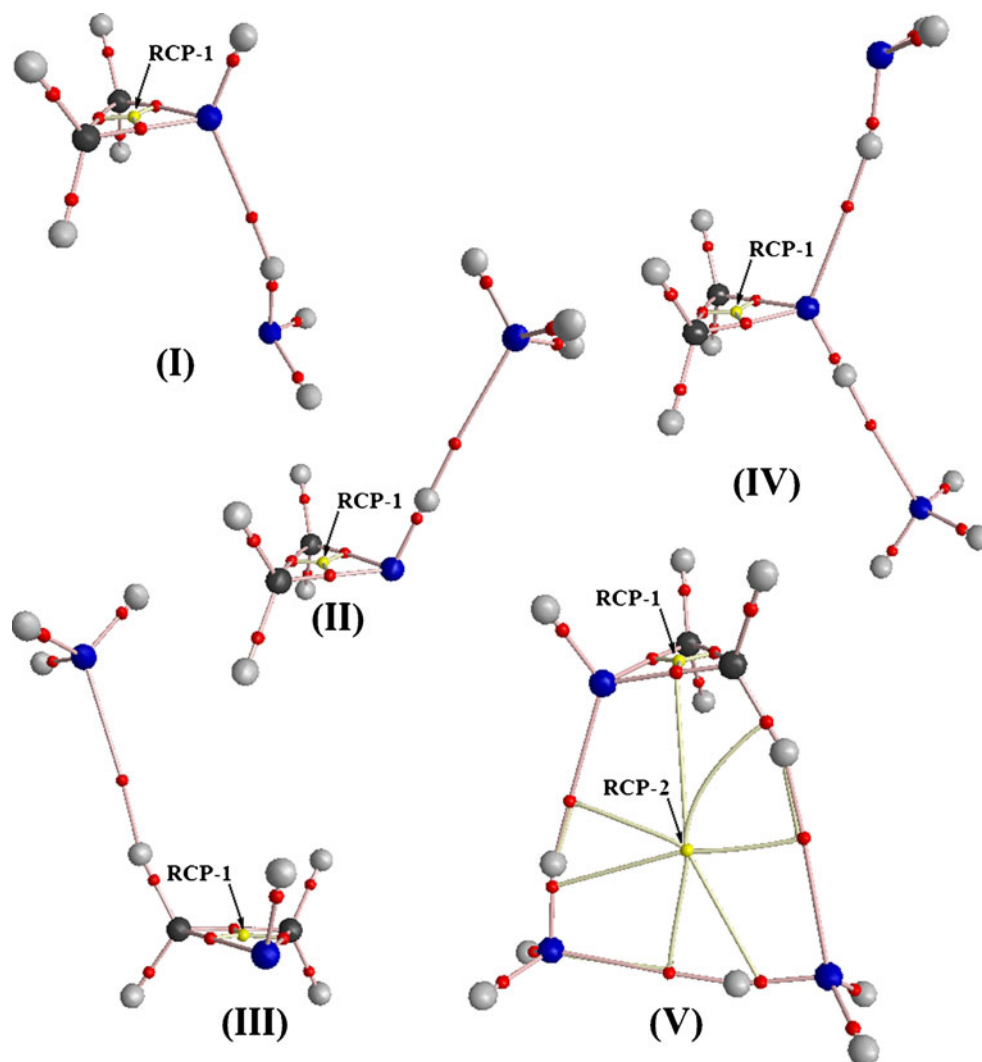
unchanged. However, it is worth pointing out that **II** and **IV** are also precedent structures of the open ring reaction,
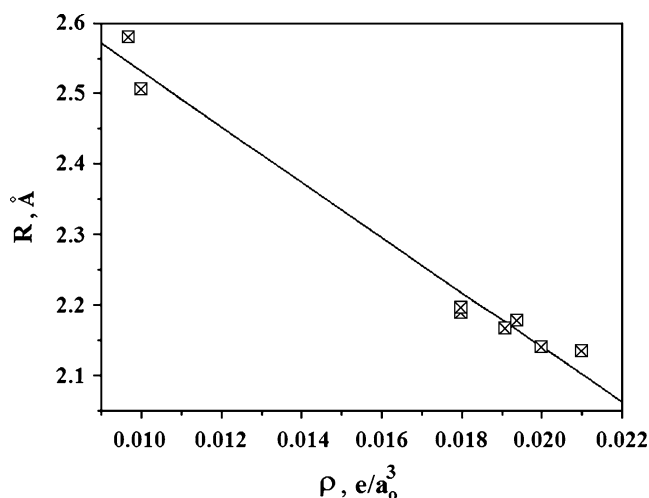
because, while the N$\cdots$H^d hydrogen bond leads to protonation of the ring in **IV**, the N$\cdots$H^c hydrogen bond captures the H^c hydrogen, which can lead to an intact aziridine ring. This hypothesis requires further investigation.

Fig. 3 Relationship between values of hydrogen bond distances R versus electronic density amounts ρ

Table 5 Values of the electronic densities ρ computed at the RCP (3,+1) of the binaries $C_2H_5N\cdots NH_3$ (I, II, and III) and ternaries $C_2H_5N\cdots 2NH_3$ (IV and V) hydrogen-bonded complexes

Systems	RCP	
	C–N–C (RCP-1)	C'–N$\cdots$H^d–N$\cdots$H^g–N$\cdots$H$^{a'}$ (RCP-2)
I	0.203	—
II	0.205	—
III	0.203	—
IV	0.204	—
V	0.202	0.002

* Values of electronic densities are given in e/a$_o^3$

* Values of electronic density at the RCP in the aziridine ring monomer is 0.204 e/a$_o^3$

Conclusions

The structures of binary and ternary hydrogen-bonded complexes formed by aziridine and ammonia were investigated. Structural results revealed typical hydrogen bond lengths, in particular deformations of the aziridine and ammonia that may indicate that they behave as donors or acceptors of protons. The hydrogen bond strength reveals that shorter interactions with lengths in the range of ~ 2 Å cause extreme modification of the monomers upon complex formation. This was confirmed by the hydrogen bond energies, whose values show that ternary hydrogen-bonded complexes are bonded more strongly, although it was not possible to reach a decisive conclusion that hydrogen bond lengths and intermolecular energies are well correlated. Nevertheless, proton donor/acceptor action has been demonstrated partially by quantification of the ChelpG charge transfer. Proton donors (**II** and **III**) and acceptors (**I**) are identified by gain and loss of charge transfer, respectively.

Spectroscopy analysis revealed good correlation between chemical shifts and hydrogen bond strength. It was also found that larger red-shifts and some blue-shifts are characteristic of proton donor interaction sites, in which the hydrogen bond energies are higher. In other words, changes in stretching frequency reveal proton donor characteristics, such as those observed in the N–H^d bonds of **I**, **IV**, and **V**. According to the results computed using QTAIM, higher intermolecular electronic densities are related to stronger hydrogen bonds. However, the relevance of the QTAIM applications is that they allow the identification of RCPs, by which ring strain can be evaluated and it becomes possible to describe the formation of the ternary hydrogen-bonded complex **V**.

References

1. Pretsch E, Bühlmann P, Badertscher M (2009) Structure determination of organic compounds. Springer, Berlin
2. Köck M, Junker J (1997) J Mol Model 3:403–407
3. Almeida MV, Assis JV, Couri MRC, Anconi CPA, Guerreiro MC, Santos HF, Almeida WB (2010) Org Lett 12:5458–5461
4. Abashkin Y, Russo N, Toscano M (1994) Int J Quantum Chem 52:695–704
5. Scott KA, Clarke J (2005) Protein Sci 14:1617–1629
6. Grzybowski BA, Bishop KJM, Kowalczyk B, Wilmer CE (2009) Nat Chem 1:31–36
7. Holubka JW, Bach RD, Andrés JL (1992) Macromolecules 25:1189–1192
8. Banks HD, White WE (2001) J Org Chem 66:5981–5986
9. Banks HD (2003) J Org Chem 68:2639–2644
10. Siddarth P, Gopinathan MS (1989) J Mol Struct (THEOCHEM) 187:169–176
11. Kim HS, Kurasawa Y, Yoshii C, Masuyama M, Takada A, Okamoto Y (1990) J Heter Chem 27:1115–1117
12. Simpson DM, Elliston JF, Katzenellenbogen JA (1987) J Steroid Biochem 28:233–245
13. Bachowska B, Zujewska T (2001) Monatsh Chem 132:849–854
14. Fazli M, Jalbout AF, Raissi H, Ghiassi H, Yoosefian M (2009) J Theor Comput Chem 8:713–732
15. Ramanathan K, Sethumadhavan R (2009) J Theor Comput Chem 8:909–924
16. Wang ZX, Duan Y (2005) J Theor Comput Chem 4:689–705
17. Jalili S, Akhavan M (2004) J Theor Comput Chem 3:527–542
18. Giese K, Lahav D, Kühn O (2004) J Theor Comput Chem 3:567–597
19. Takahashi O, Kohno Y, Nishio M (2010) Chem Rev 110:6049–6076
20. Oliveira BG, Araújo RCMU, Carvalho AB, Ramos MN (2011) J Mol Model 17:2847–2862
21. Rehm TH, Schmuck C (2010) Chem Soc Rev 39:3597–3611
22. Oliveira BG, Araújo RCMU (2011) Monatsh Chem 142:861–873
23. Grabowski SJ (2011) Chem Rev 111:2597–2625
24. Elguero J, Katritzky AR, Denisko OW (2000) Adv Heter Chem 76:157–323
25. Oliveira BG, Araújo RCMU, Carvalho AB, Ramos MN (2009) Struct Chem 20:663–670
26. Gadzhiev BO, Ignatov SK, Razuvaev AG, Masunov AE (2009) J Phys Chem A 113:9092–9101
27. Oliveira BG, Araújo RCMU, Chagas FF, Carvalho AB, Ramos MN (2008) J Mol Model 14:949–955
28. Oliveira BG, Araújo RCMU, Ramos MN (2008) Struct Chem 19:665–670
29. Oliveira BG, Araújo RCMU, Silva JJ, Ramos MN (2010) Struct Chem 21:221–228
30. Oliveira BG, Vasconcellos MLAA (2009) Inorg Chem Commun 12:1142–1144
31. Jursic B (1998) J Mol Struct (THEOCHEM) 434:37–42
32. Grabowski SJ, Bilewicz E (2006) Chem Phys Lett 427:51–55
33. Grabowski SJ, Leszczynski (2009) J Chem Phys 355:169–176
34. Biczysko M, Latajka Z (1999) Chem Phys Lett 313:366–373
35. Oliveira BG, Araújo RCMU, Carvalho AB, Lima EF, Silva WLV, Ramos MN, Tavares AM (2006) J Mol Struct (THEOCHEM) 775:39–45
36. Oliveira BG, Araújo RCMU, Pereira FS, Lima EF, Silva WLV, Carvalho AB, Ramos MN (2008) Quim Nova 31:1673–1679
37. Giuliano BM, Castrovilli MC, Maris A, Melandri S, Caminati W, Cohen EA (2008) Chem Phys Lett 463:330–333
38. Rensing C, Mäder H, Temps F (2008) J Mol Spec 251:224–228
39. Oliveira BG, Santos ECS, Duarte EM, Araújo RCMU, Ramos MN, Carvalho AB (2004) Spectrochim Acta A 60:1883–1887
40. Oliveira BG, Duarte EM, Araújo RCMU, Ramos MN, Carvalho AB (2005) Spectrochim Acta A 61:491–494
41. Oliveira BG, Araújo RCMU (2007) Quim Nova 30:791–796
42. Kaur D, Khanna S (2011) Comput Theor Chem 963:71–75
43. Zabardasti A, Amani S, Solimannejad M, Salehnassaj M (2009) Struct Chem 20:1087–1092
44. Li J (2006) J Theor Comput Chem 5:187–196
45. Vasconcellos MLAA, Oliveira BG, Leite LFCC (2008) J Mol Struct (THEOCHEM) 860:13–17
46. Geerlings P, De Proft F, Langenaeker W (2003) Chem Rev 103:1793–1873
47. Kolboe S, Svelle S (2008) J Phys Chem A 112:6399–6400
48. Riley KE, Pitonak M, Cerny J, Hobza P (2010) J Chem Theor Comput 6:66–80

49. Oliveira BG, Araújo RCMU, Ramos MN (2009) J Mol Struct (THEOCHEM) 908:79–83
50. Rao L, Ke H, Fu G, Xu X, Yan Y (2009) J Chem Theor Comput 5:86–96
51. Oliveira BG, Vasconcellos MLAA (2009) Struct Chem 20:897–902
52. Oliveira BG, Araujo RCMU, Carvalho AB, Ramos MN (2007) Quim Nova 30:1167–1170
53. Oliveira BG, Araujo RCMU, Carvalho AB, Ramos MN, Hernandes MZ, Cavalcante KR (2007) J Mol Struct (THEOCHEM) 802:91–97
54. Guerra CF, Baerends EJ, Bickelhaupt FM (2006) Int J Quantum Chem 106:2428–2443
55. Araújo RCMU, Silva JBP, Ramos MN (1995) Spectrochim Acta A 51:821–830
56. Araújo RCMU, Ramos MN (1996) J Mol Struct (THEOCHEM) 366:233–240
57. Araújo RCMU, Ramos MN (1998) J Braz Chem Soc 9:499–505
58. Wolk JL, Rozental E, Basch H, Hoz S (2006) J Org Chem 71:3876–3879
59. Tokura S, Tsuneda T, Hirao K (2006) J Theor Comput Chem 5:925–944
60. Kageura Y, Sakota K, Sekiya H (2009) J Phys Chem A 113:6880–6885
61. Bader RFW (1990) Atoms in molecules a quantum theory. Clarendon, Oxford
62. Bader RFW (1991) Chem Rev 91:893–928
63. Filho EBA, do Monte EV, do Monte S, Oliveira BG, Junior CGL, Rocha GB, Vasconcellos MLAA (2007) Chem Phys Lett 449:336–340
64. Sokol W, Werstiuk NH (2008) Can J Chem 86:737–744
65. Huang Z, Yu L, Daí Y, Wang H (2011) Struct Chem 22:57–67
66. Kudin KN, Strain MC, Farkas O, Tomasi J, Barone V, Cossi M, Cammi R, Mennucci B, Pomelli C, Adamo C, Clifford S, Ochterski J, Petersson GA, Ayala PY, Cui Q, Morokuma K, Rega N, Salvador P, Dannenberg JJ, Malick DK, Rabuck AD, Raghavachari K, Foresman JB, Cioslowski J, Ortiz JV, Baboul AG, Stefanov BB, Liu G, Liashenko A, Piskorz P, Komaromi I, Gomperts R, Martin RL, Fox DJ, Keith T, Al-Laham MA, Peng CY, Nanayakkara A, Challacombe M, Gill PMW, Johnson B, Chen W, Wong MW, Andres JL, Gonzalez C, Head-Gordon M, Replogle ES, Pople JA (1998) Gaussian 98W Revision A.1. Gaussian Inc, Pittsburgh
67. van Duijneveldt FB, Murrell JN (1967) J Chem Phys 46:1759–1767
68. Boys SB, Bernardi F (1970) Mol Phys 19:553–566
69. McQuarrie DA (1973) Statistical thermodynamics. Harper and Row, New York
70. Cioslowski J, Stefanov BB (1996) Chem Phys Lett 256:449–453
71. AIM 2000 1.0 program designed by Biegler-König F, University of Applied Sciences, Bielefeld, Germany
72. Breneman CM, Wiberg KB (1990) J Comput Chem 11:361–373
73. Oliveira BG, Pereira FS, Araújo RCMU, Ramos MN (2006) Chem Phys Lett 47:181–184
74. Oliveira BG, Lima MCA, Pitta IR, Galdino SL, Hernandes MZ (2010) J Mol Model 16:119–127
75. Padwa A (2008) Comp Heter Chem 18:1–197
76. Epshtein LM (1979) Russ Chem Rev 48:854–867
77. Zefirov YV, Zorky PM (1995) Russ Chem Rev 64:415–428
78. Wiberg KN (2004) Found Chem 6:65–80
79. Cremer D, Kraka E (1985) J Am Chem Soc 107:3800–3810
80. Cremer D, Kraka E (1985) J Am Chem Soc 107:3811–3819
81. Oliveira BG, Araújo RCMU, Ramos MN (2010) J Mol Struct (THEOCHEM) 944:168–172
82. Oliveira BG, Ramos MN (2010) Int J Quantum Chem 110:307–316
83. Umeyama H, Morokuma K (1977) J Am Chem Soc 99:1316–1332
84. Bleiholder C, Werz DB, Köppel H, Gleiter R (2006) J Am Chem Soc 128:2666–2674
85. Pichlmaier M, Winter RF, Zabel M, Záliš S (2009) J Am Chem Soc 131:4892–4903
86. Araújo RCMU, Soares VM, Oliveira BG, Lopes KC, Ventura E, Monte S, Santana O, Carvalho AB, Ramos MN (2006) Int J Quantum Chem 106:2714–2711
87. Oliveira BG, Araújo RCMU, Soares VM, Ramos MN (2008) J Theor Comput Chem 7:245–256
88. Znamenskiy YS, Gree ME (2007) J Chem Theor Comput 3:103–114
89. Hohenstein EG, Sherrill CD (2011) Wavefunction methods for noncovalent interactions. Interdisciplinary Reviews: Computational Molecular Science. Wiley, New York
90. Stone AJ, Misquitta AJ (2009) Chem Phys Lett 473:201–205
91. Rusu VH, Ramos MN, Silva JBP (2006) Int J Quantum Chem 106:2811–2817
92. Nesbitt DJ (1988) Chem Rev 88:843–870
93. Oliveira BG, Araújo RCMU, Carvalho AB, Ramos MN (2009) J Mol Model 15:123–131
94. Barnes AJ (2004) J Mol Struct 704:3–9
95. Yu W, Lin Z, Huang Z (2006) Chem Phys Chem 7:828–830
96. Dhumal NR, Gejji SP (2004) Chem Phys Lett 393:355–360
97. Joseph J, Jemmis ED (2007) J Am Chem Soc 129:4620–4632
98. Scheiner S, Kar T (2002) J Phys Chem A 106:1784–1789
99. Herrebout WA, Delanoye SN, van der Veken BJ (2004) J Phys Chem 108:6059–6064
100. Popelier PLA (2000) Atoms in Molecules. An Introduction. Pearson, Harlow, UK
101. Matta CF, Boyd RJ (2007) The quantum theory of atoms in molecules: from solid state to DNA and drug design. Wiley-VCH, Weinheim
102. Matta CF (2009) Quantum biochemistry: electronic structure and biological activity. Wiley-VCH, Weinheim
103. Popelier PLA (2000) Coord Chem Rev 197:169–189
104. Bader RFW (2005) Monatshefte für Chemie 136:819–854
105. Okulik N, Jubert AH, Castro EA (2002) J Mol Struct (THEOCHEM) 589–590:79–87
106. Alsberg BK, Marchand-Geneste N, King RD (2000) Chemom Intell Lab Syst 54:75–91
107. Oliveira BG, Vasconcellos MLAA (2006) J Mol Struct (THEOCHEM) 774:83–88
108. Oliveira BG, Leite LFCC (2008) J Mol Struct (THEOCHEM) 915:38–42
109. Oliveira BG, Araújo RCMU, Ramos MN (2007) Chem Phys Lett 433:390–394
110. Oliveira BG, Vasconcellos MLAA, Olinda RR, Filho EBA (2009) Struct Chem 20:81–90
111. Oliveira BG, Araújo RCMU, Ramos MN (2010) Quim Nova 33:1155–1162
112. Desiraju GR (2010) Angew Chem Int Edn 49:2–10
113. Castillo N, Matta CF, Boyd RJ (2005) Chem Phys Lett 409:265–269
114. Grabowski SJ (2004) Monatsh Chem 133:1373–1380